Magnetic coupling and spin structure in nanocrystalline iron powders

2006 J. Phys.: Condens. Matter 18 2235

(http://iopscience.iop.org/0953-8984/18/7/011)

INSTITUTE OF PHYSICS PUBLISHING JOURNAL OF PHYSICS: CONDENSED MATTER

J. Phys.: Condens. Matter **18** (2006) 2235–2248 doi:10.1088/0953-8984/18/7/011

Magnetic coupling and spin structure in nanocrystalline iron powders

A Ślawska-Waniewska[1], M Grafoute[2] and J M Greneche[2,3]

[1] Institute of Physics, Polish Academy of Sciences, Aleja Lotnikow 32/46,02-668 Warsaw, Poland
[2] Laboratoire de Physique de l'Etat Condensé, UMR CNRS 608, Université du Maine, 72085 Le Mans Cedex, France

E-mail: greneche@univ-lemans.fr

Received 28 October 2005, in final form 9 January 2006
Published 2 February 2006
Online at stacks.iop.org/JPhysCM/18/2235

Abstract

Pure single-phase iron nanostructured particles with pseudo-cubic shape crystalline grains and linear dimensions of around 11 nm can be produced by the low energy ball milling of microcrystalline Fe under argon atmosphere. The long range ferromagnetic correlation of exchange coupled crystallites extending across grain boundaries leads to a reduction of the effective anisotropy, as expected from the generalized random anisotropy model. This ferromagnetic network of correlated grains is preserved at low temperatures. No spin-glass freezing process is detected. Slight oxidation of the particles with formation of an FeO phase is achieved with deliberately prolonged milling. This FeO phase leads to non-collinear spin structure at the interfaces that suppresses the intergrain correlations and enhances the role of long range dipolar interactions. The interface spin disorder and the complex state of the intergrain interactions are the sources of the spin-glass-like behaviour found in these Fe–FeO nanocomposites.

(Some figures in this article are in colour only in the electronic version)

1. Introduction

In the last decade nanogranular materials have attracted a great deal of interest due to their non-conventional physical, chemical and magnetic properties. In contrast to the case for microcrystalline systems, a large fraction of their atoms are located in the grain boundaries (or intergranular phase), characteristic of materials with an enhanced surface to volume ratio [1–4]. The structures of ultrafine grains result from both (i) their reduced sizes which are in the nanometre range and (ii) grain boundaries. Their magnetic properties are additionally modified

[3] Author to whom any correspondence should be addressed.

by the interactions between the grains and between the grains and grain boundaries; see e.g. ([5] and references therein). More recent studies have shown that nanostructured materials exhibit a reduced density which is mainly due to a wide distribution of interatomic distances between nearest neighbour atoms in the grain boundaries [1, 4]. Thus the nanograins are often considered as composed of two phases—core and shell—each of which exhibits different properties [5–11]. One of the most widely studied systems is the metallic Fe nanoparticles. In most cases, for environmental stability, these particles were passivated with thin layers of iron oxides. The magnetic properties of oxide coated Fe grains form the subject of many papers [6–14]. It is generally agreed that in granular systems with the core–shell morphology, the disordered oxide layers exhibit a spin-glass-like behaviour [3, 5, 8–11]. Much less is known about single-phase Fe particles. Investigations of Fe grains crystallized inside the amorphous FeZrCuB matrix revealed the presence of grain boundaries with non-collinear spin structures [15]. Subsequently, for ball milled nanocrystalline Fe, fcc structure [16] and spin-glass-like behaviour [17] of the grain boundaries were reported. These latter results led Del Bianco *et al* [33] to a generalization and statement that as-milled nanopowders are two-phase materials (composed of crystalline regions and grain boundaries) and that the low temperature frozen disordered state is inherently connected to the nanocrystalline character and is due to the large fraction of the disordered grain boundaries [33]. At this point it must be noted that in this case the samples were prepared and handled in air [16], which certainly causes oxidation of the as-milled particles which can even proceed further over time, as was demonstrated by Linderoth *et al* [9]. Moreover, the effects of possible impurities, Cr in particular, were not considered, although, as was shown by Balogh *et al* [19], they, rather than the grain boundary phase, could be responsible for certain features of the hyperfine field distribution. Consequently, some grain boundaries were identified for the Fe powder milled for 160 h under vacuum, although in this case Cr impurities from the steel milling tools were introduced into the intergrain interfaces [12].

One can find in the literature different results on the same system reported by different groups of researchers as well as contradictory interpretations of some of them. In view of the doubts related to some experimental findings, we aimed in the present work to study nanostructured Fe powders with special care devoted to both the preparation and the storage conditions, in order to reduce possible surface contamination and/or oxidation processes. This is motivated by the desire to obtain pure single-phase Fe particles where, unlike for the widely studied Fe/Fe oxide systems, the chemistry and structure of the grain boundaries would be as similar as possible to those of Fe cores. For these studies, the nanostructured powders were produced by the high energy ball milling technique. It is well established that the type of milling and the processing parameters used significantly affect the resulting microstructures and nanostructures of both crystalline grains and grain boundaries [18]. Indeed, during ball milling, a steady state grain size can be reached when the powder is milled for a certain period of time. An extension of the milling time cannot be used to decrease the grain size further. Nevertheless, contamination is obviously inevitable when the powder undergoes a long period of milling. As the grain boundaries constitute a significant component in nanostructured materials, it is then important to emphasize that the impurity and the impurity-containing phases are generally concentrated in the interface [12, 18, 19]. But it is usually a very difficult task to separate those impurities from the grain boundaries. Both factors affect the magnetic behaviour of granular nanostructures, which are the source of surface anisotropy but also essentially modulate the couplings between the grains that occur across the interface.

In this paper, the properties of the grain boundaries as well as the magnetic interparticle correlations across the grain boundaries are investigated by several complementary experimental techniques. All the samples were prepared under high vacuum conditions to avoid

contaminations and/or post-preparation oxidation. The structural models of the ball milled Fe powders are discussed and related to their magnetic behaviour. Analysis is performed within the generalized random anisotropy approach that takes into account the possible reduced intergrain exchange coupling across the grain boundaries.

2. Experimental procedure

Microcrystalline iron (purity ∼99.95%), with particle sizes 1–2 μm, was milled in a commercial Fristsch Pulverisette 7 planetary ball mill with hardened steel balls 12 mm of diameter at room temperature. The ball to powder weight ratio was 10 to 1. The set was charged into the vial. It is well established that some of the relevant parameters of the milling conditions have a significant effect on the grain size (milling speed, milling time) while other parameters contribute to contamination of powders (milling atmosphere, nature of balls and mill vial) [20, 21]. Consequently, the loading was done in a glove box under an argon atmosphere, and two different milling intensities were considered by varying the rotation velocity of the milling plate. The powders obtained were analysed by means of electron dispersive x-ray spectroscopy. Indeed, the analysis of high energy ball milled Fe powders (velocity $I = 10$; rotation of the vial 1400 tr min^{-1}) reveals the presence of Cr, as predicted by Balogh *et al* [12, 19], the content of which was increasing with the milling time. In contrast, no presence of Cr was evidenced in the low energy ball milled Fe powder (velocity $I = 6$; rotation of the vial 800 tr min^{-1}). This is in agreement with Balogh *et al* [19] who also found that for milling time below 100 h, Cr contamination could be negligible. Thus, the present study is focused on low energy milled samples obtained for the milling times $t_m = 1$, 16, 32, 48 and 64 h; the milling process was interrupted for 15 min h^{-1} in order to stabilize the temperature in the vial. To avoid oxidation, the as-milled powders were protected from the air and the samples were prepared under high vacuum and for further studies placed in hermetically sealed capsules.

X-ray diffraction (XRD) patterns were obtained using a Phillips X'pert diffractometer with tension 40 kV and intensity 30 mA. A wavelength of $\lambda = 1.5405$ Å was used to obtain data in the range $20° < 2\theta < 120°$, in steps of 0.04°. To get an extremely high statistics pattern a long registration time (about 60 h) was used. The powdered sample was located in a special chamber preventing any oxidation during the measurements. The structural and microstructural parameters were refined from the x-ray pattern using the MAUD [22] procedure which is based on the Rietveld method combined with Fourier analysis: the crystalline grain size and the microstrain were evaluated by means of the Warren–Averbach procedure. The morphology of particles was followed as a function of milling time using a scanning electron microscope while the presence of contaminant elements was controlled by means of electron dispersive x-ray spectroscopy.

The Mössbauer spectra of the samples milled for different times have been carefully measured in a standard transmission geometry using a conventional spectrometer with a constant acceleration signal and a ^{57}Co source diffused into a rhodium matrix. The samples, which consisted of 5 mg cm^{-2} of milled Fe mixed with dried AlF_3 (under a controlled atmosphere to prevent oxidation) were placed into a cryostat under vacuum, allowing us thus to perform measurements over the temperature range 4.2–300 K. The dc magnetization measurements were performed with a vibrating sample magnetometer (Oxford Instruments Ltd) in the field range ±1.1 T, whereas the ac measurements were performed with an ac susceptometer (Oxford Instruments Ltd); in both cases they were performed under vacuum over the temperature range 4–300 K.

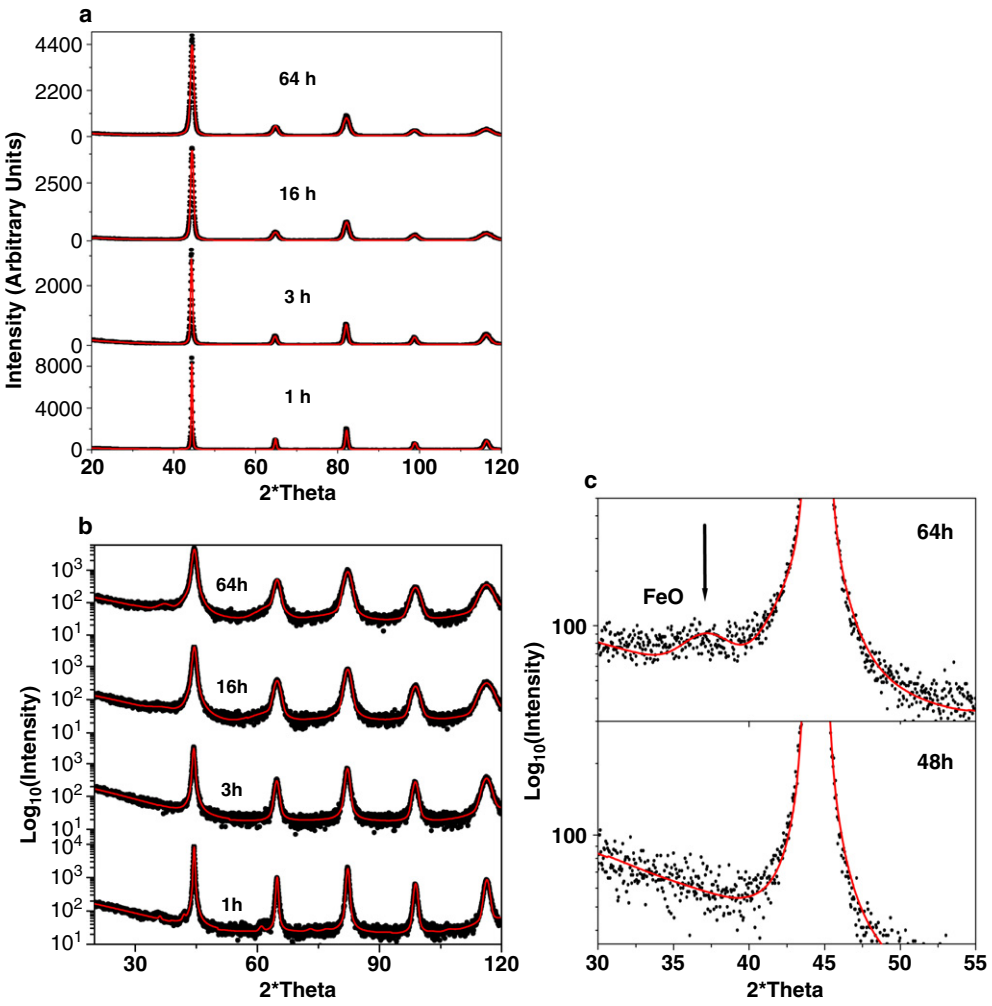

Figure 1. X-ray diffraction patterns of iron powders for different milling times with a linear (a) and logarithmic (b) intensity scale; (c) details the shoulder of the main Bragg peak.

3. Experimental results

3.1. X-ray diffractometry

X-ray diffraction patterns of Fe powders milled for different times are presented in figure 1; they exhibit peaks clearly attributable to bcc Fe, which broaden with the increase of the milling time. For better clarity, the fitted patterns are plotted using both linear and logarithmic intensity scales (figures 1(a) and (b), respectively), showing thus to what extent the low part of the Bragg peaks is well reproduced. Different fitting models were proposed assuming a single component with (i) spherical structural domains, (ii) anisotropic shape of structural domains. For milling times longer than 16 h, the best refinement was achieved assuming the presence of structural domains with a pseudo-cubic shape, as shown in figure 2. The dependence of the mean grain size obtained as a function of the milling time is plotted in figure 3. It is seen that at an early stage of the mechanical attrition, the average structural domain size decreases sharply while the

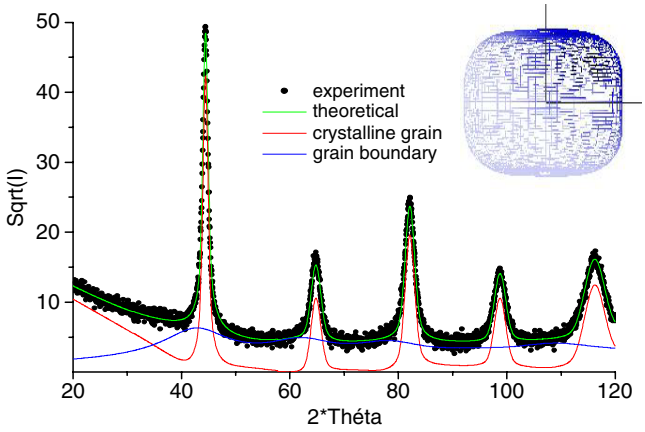

Figure 2. X-ray pattern of the sample milled for 32 h fitted with two components and pseudo-cubic crystalline grains (see the details in the inset).

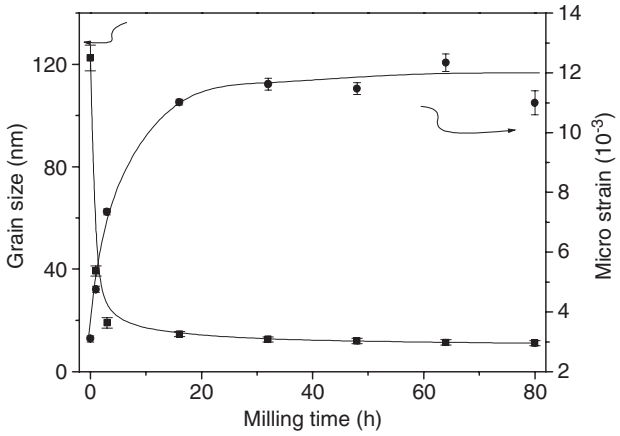

Figure 3. Average grain size and microstrain for milled Fe powders versus milling time.

microstrain increases quite rapidly and both reach relatively quickly a steady state. After 32 h milling, the average grain size is 11 ± 2 nm. This is fairly consistent with that characteristic of the milled iron powder reported in the literature (8–13 nm) [16, 21, 23].

For powder milled for at least 32 h, i.e. in the steady state, we can therefore consider a description in terms of two components: one attributed to crystalline grains (as before) and the other to the grain boundaries. This latter component is characterized by a very small coherent structural length of about 0.4 nm suggesting a topological atomic disorder—such a description has been earlier proposed in the case of nanostructured powders of ferric fluorides [24, 25]. The relative content of this component is about 12% in the Fe milled powders studied. Assuming a dense random packing of cubic shaped grains, this value allows us to estimate the thickness of the grain boundary at about 0.8 nm, i.e. 2–3 atomic layers. Finally, in the x-ray pattern of the 64 h milled powder (figure 1(c)), some traces of Fe oxide FeO (wüstite) are seen (up to 3 at.%). It seems that FeO is a preferential oxide formed during prolonged processing, since even milling of $Fe_2O_3 + Fe$ for a certain time leads to the formation of FeO + Fe, as shown by Ding *et al* [26]. Although for shorter milling times neither Fe oxides or impurity phases were

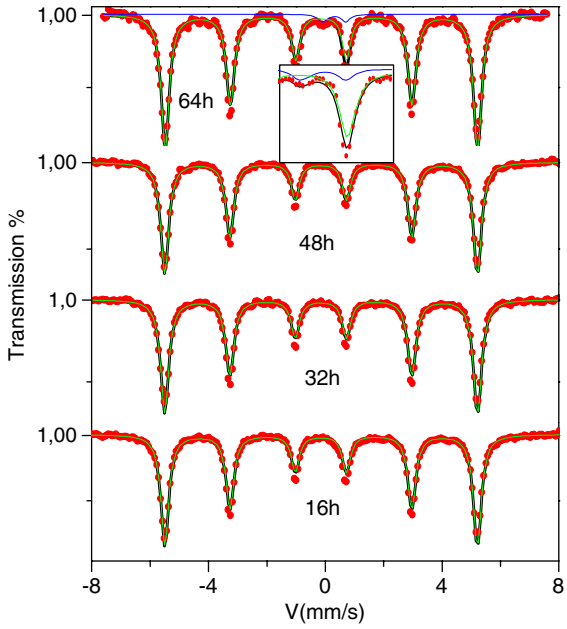

Figure 4. Room temperature Mössbauer spectra of the samples milled for 16, 32, 48 and 64 h. The inset shows the presence of the quadrupolar doublet due to the wüstite.

Table 1. Mössbauer parameters of the powders milled for different times: linewidth, B_{hf} (hyperfine field), IS (isomer shift) and the fraction of FeO phase.

Milling time (h)	Linewidth (mm s^{-1}) ±0.005	B_{hf} (T) ±0.1	IS (mm s^{-1}) ±0.003	FeO (%) ±1
16	0.340	33.0	0.005	0
32	0.340	33.0	0.004	0
48	0.342	33.0	0.002	0
64	0.344	33.0	0.007	3

detected by x-ray studies; however, traces of oxidation and some contaminations (both below the sensitivity limits of the techniques applied) cannot be excluded.

3.2. ^{57}Fe Mössbauer spectrometry

Mössbauer spectra of samples milled for 16, 32, 48 and 64 h have been recorded at 300 K (figure 4) and at 77 K (not shown, because they are very similar). They exhibit sextets with well defined lines. Unlike in previous studies [1, 10, 16–18, 27], the fitting is well achieved (profile and intensity of each line) by considering a single magnetic component with Lorentzian lines, the linewidth of which remains quite small at both 77 and 300 K. It is important to emphasize that a model involving a hyperfine field distribution (as in [10] and [16]) does not improve the quality of the fit but gives rise to a prevailing single peak. The refined values of hyperfine parameters at 300 K, which are listed in table 1, agree with those of metallic bcc Fe. For 64 h milled powder the presence of a small quadrupolar contribution (see the inset of figure 4) which disappears at 77 K is found; this component is attributed to the small admixture of the wüstite (FeO), which behaves as an antiferromagnet with the Néel temperature of about 200 K, which is in agreement with x-ray data.

At this stage, it should be mentioned that Mössbauer spectrometry, despite its high sensitivity to the local order, does not provide any relevant information on the presence of grain

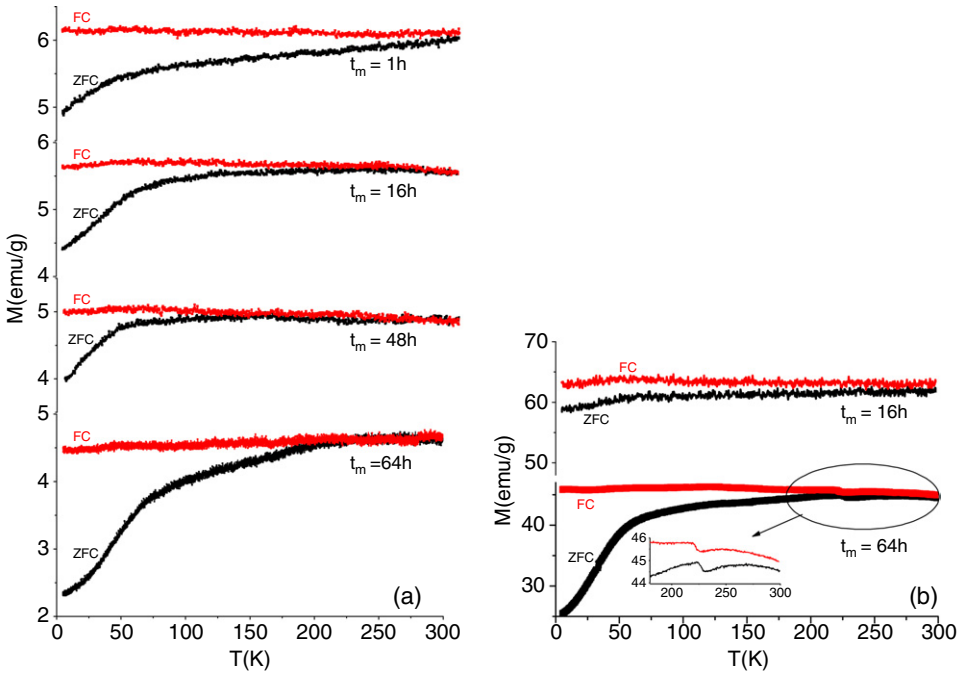

Figure 5. Temperature dependences of the magnetization measured in zero-field cooled (ZFC) and field cooled (FC) conditions at the applied field of 50 Oe for all the samples studied (a) and at 500 Oe for the sample milled for 16 and 64 h (b).

boundaries in the samples studied. As the hyperfine field is not affected and remains similar to that of crystalline grains at both 300 and 77 K, it can be suggested that the grain boundaries are only weakly disordered and quite narrow (in agreement with x-ray description: 2–3 atomic layers). High temperature could eventually cause a splitting of the hyperfine structure and high temperature measurements could then differentiate between the core and shell phases, but simultaneously the long registration time may cause a structural transformation of the powder, including a transition from the nanocrystalline state to the microcrystalline one.

3.3. The dc and ac magnetic measurements

The temperature dependences of the magnetization have been measured in the zero-field cooled (ZFC)–field cooled (FC) regime over the temperature range 4.2–300 K in the applied fields of 50 and 500 Oe. The ZFC magnetization curve was obtained after cooling the demagnetized sample in zero field and then by measuring the sample magnetization with increasing temperature in a small external field. The FC magnetization was also measured on warming but after cooling the sample in the same small applied field. The results obtained at 50 Oe are shown in figure 5(a). The ZFC–FC curves exhibit irreversibility (a split between ZFC and FC branches) over the whole temperature range and their evolutions indicate the existence of strong interparticle interactions in all the as-milled samples. In the ZFC curves two parts with different slopes can be distinguished: a strong increase from 4 to ∼70 K followed by a much weaker increase of magnetization with the temperature rise. In turn, FC curves remain roughly constant over the whole temperature range studied. Increasing the milling time up to 48 h, a gradual reduction in the ZFC–FC irreversibility is observed, but further increase of the

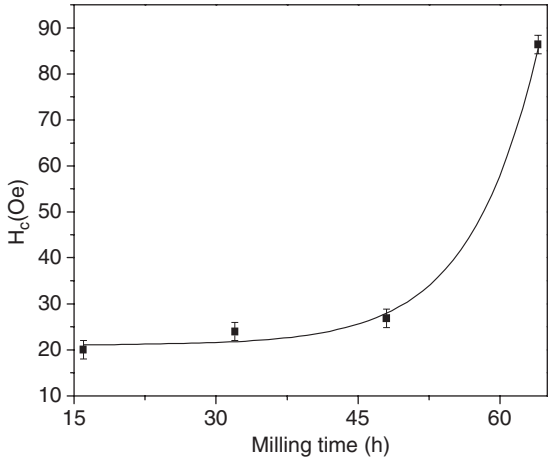

Figure 6. Evolution of the coercive field with the milling time.

milling time (up to 64 h) results in a suppression of this tendency, a sudden increase of the irreversibility and a change of the shape of the ZFC curve. For shorter milling times the low temperature irreversibility depends on the field applied and it practically disappears at 500 Oe, as shown in figure 5(b) for the sample milled for 16 h.

For all the samples studied the hysteresis loops were recorded at selected temperatures. In the as-milled powders the room temperature value of the coercivity is small (∼20 Oe) and does not essentially change with the milling time up to 48 h of milling, as shown in figure 6. The magnetic hardening of the Fe nanopowder is observed for longer milling time. The samples obtained up to 48 h of milling show a gradual increase of H_c and M_r with decreasing temperature; the example data obtained for the 48 h sample are shown in figure 7(a). This behaviour changes for the sample milled for 64 h, where maxima in both the $H_c(T)$ and $M_r(T)$ dependences are observed at around 25 K—figure 7(b). Moreover, for this sample at 5 K both a broadening of the loop and a shift to the negative field side occur when the cooling is performed in the external field of 1 T, whereas such an effect is not observed for the other samples.

For the 64 h milled sample the range of the ZFC–FC low temperature irreversibility does not strongly depend on the field applied and the curves obtained in 500 Oe scale roughly with the field in relation to those measured at 50 Oe, as shown in figure 5(b). The most pronounced effect of the higher applied field is a reduction of the temperature at which the change of slope in ZFC curve occurs—from ∼75 K (for 50 Oe) to ∼60 K (for 500 Oe). This temperature matches up to the change of slope of the thermoremanent magnetization TRM curve (measured on warming after cooling the sample in a magnetic field of 1 T down to 4 K, at which the field was removed), as shown in figure 9. For this sample the real and imaginary components of the ac susceptibility were also measured and the results obtained at the frequency of 1 kHz are presented in figure 8. Although a continuous increase of the real component of the susceptibility is seen with the temperature rise, for the imaginary part a well defined peak at 75 K is observed. For the other samples the susceptibility measurement did not reveal any low temperature peak.

4. Discussion

The nanosize iron powder can be created by low energy milling of the microcrystalline Fe under an argon atmosphere. For milling time longer than 10 h a steady state is achieved where the average grain sizes and microstrains remain roughly constant. The results obtained indicate

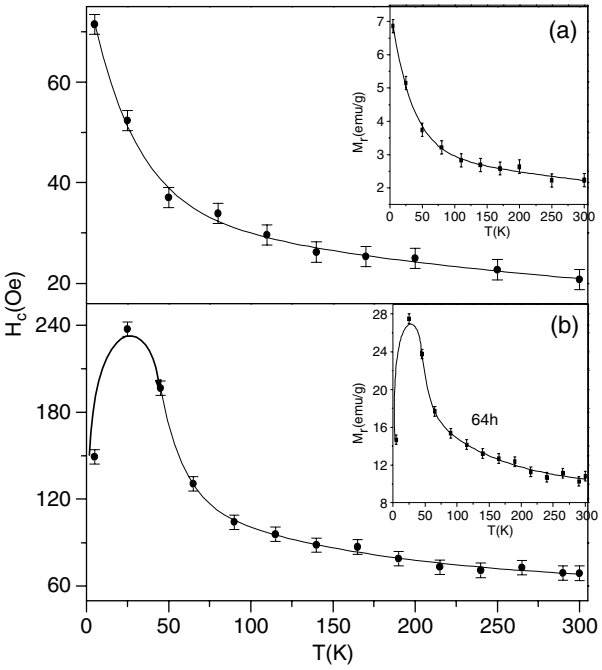

Figure 7. Temperature dependences of the coercivity for the samples milled for 48 h (a) and 64 h (b); the inset shows the remanence versus temperature for the corresponding samples (lines are guides for the eyes).

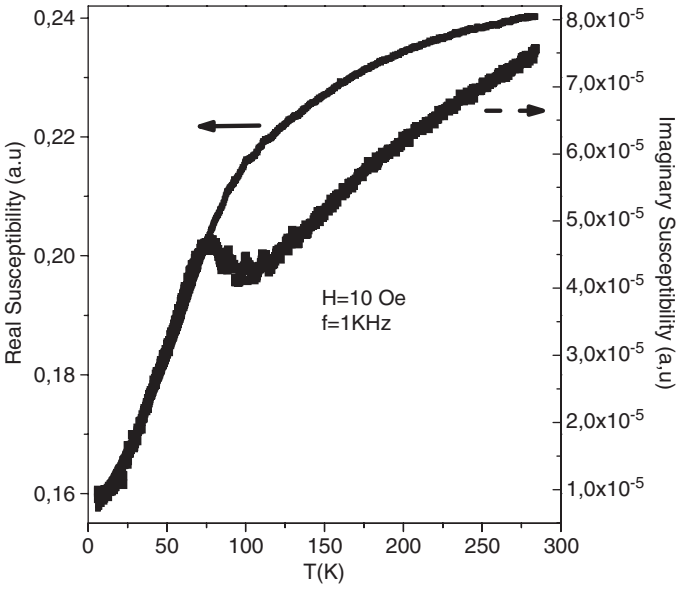

Figure 8. Thermal evolution of the real and imaginary components of the ac susceptibility for the sample milled for 64 h.

that for Fe nanostructured powders in the steady state range ($t_m > 10$ h) two different stages and corresponding magnetic properties are observed: (1) for the milling time up to 48 h, where the sample can be considered as partly inhomogeneous pure iron systems, and (2) for longer milling time (64 h), where the additional FeO phase is formed and affects the overall magnetic behaviour of the powder. These two cases are discussed separately.

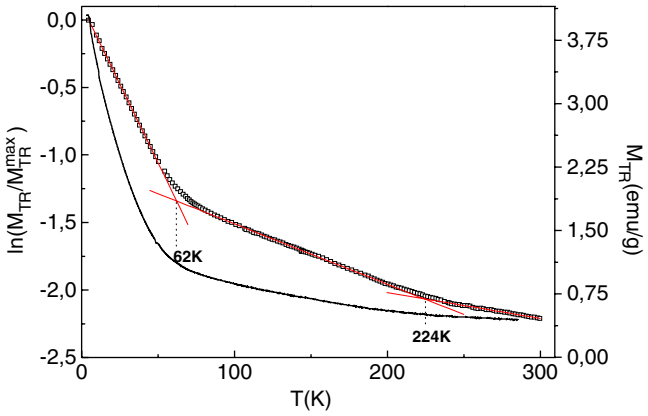

Figure 9. The thermoremanent magnetization M_{TR} (right axis) collected after cooling the sample at 1 T and a semi-logarithmic plot of the normalized thermoremanent magnetization (left axis) versus temperature; straight lines indicate three regimes of the exponential decay.

4.1. Pure nanocrystalline Fe systems ($48\ h \geqslant t_m > 10\ h$*)*

The as-milled nanostructured powders, which are composed of agglomerates of randomly oriented iron grains, can be characterized by the structural and hyperfine parameters typical of bulk Fe. The grains are separated by a thin interfacial layer where the coherent structural length is small but the nearest neighbour surrounding of Fe atoms remains the same as inside the grains and thus this phase cannot be distinguished in the Mössbauer spectra. This indicates that when the interfacial layer is thin and its chemistry is the same as that inside the grain, the proximity effect of neighbouring grains and strong exchange coupling between Fe atoms from neighbouring particles cause an apparent increase of the coordination number of surface Fe atoms leading to the hyperfine parameters being very similar to those of the crystalline interior. The samples behave as strongly correlated ferromagnets and their magnetic behaviour is dominated by interparticle interactions. They exhibit soft magnetic behaviour and their coercivity observed at room temperature is very small (∼20 Oe), even smaller than that for the microcrystalline precursor (∼35 Oe). It has to be noted that although nanocrystalline iron has been intensively investigated, in most cases the particles studied exhibited a core–shell structure with the shell formed by iron oxide(s) [5–14]. The coercivity of agglomerates of particles 10–15 nm in diameter reaches hundreds of Oe [6, 7, 11, 28–30], that is at least one order of magnitude larger than that found in this paper. The coercivity of 20 Oe observed for the as-milled powder is also smaller than the value obtained from the Stoner–Wohlfarth model for spherical single-domain Fe particles (∼180 Oe at 300 K) [13]. For iron nanocrystalline particles (10–15 nm of diameter) such small values of the coercivity as well as a similar temperature dependence of the coercivity have only been observed for as-prepared particles produced by the inert gas condensation technique and consolidated at 1.2 GPa for 2 h under vacuum [13].

The magnetic softness of agglomerated particles in as-milled powders arises from strong interparticle exchange interactions which extend across the interfaces. This can be explained within the generalized random anisotropy model (that includes the reduction of intergrain coupling due to the presence of a disturbed interface) proposed by Löffler *et al* [31]. According to this model, the exchange correlation length L, which results from the balance between the anisotropy energy of the individual grain and the exchange energy required for adjusting the magnetization between the grains, has the proportionality

$$L \sim (A_{\mathrm{eff}}/K)^2 D^{-3}, \tag{1}$$

where D is the average grain size, K is the anisotropy constant and A_{eff} is the effective exchange

constant, which for cubic grains can be expressed as

$$A_{\mathrm{eff}} = A_{\mathrm{b}}(1 + d/D)/(1 + A_{\mathrm{b}}d/A_{\mathrm{in}}D), \tag{2}$$

where A_{b} is the bulk exchange stiffness constant, A_{in} characterizes the reduced exchange across the interfaces and d is the width of the interface [31]. For nanostructured iron with grain sizes of 10 and 15 nm this model predicted that the magnetic exchange correlation length is about 60 and 190 nm, respectively [31]. The intergrain correlations which extend over hundreds of crystalline grains lead thus to an appreciable reduction of the effective anisotropy in the as-milled samples and, consequently, a small coercivity. It should be noted that the generalized random anisotropy model is especially suitable for the interpretation of the experimental results presented in this paper. The effective exchange constant obtained there (equation (2)) was calculated for the cubic grains and can thus well approximate the interactions between the pseudo-cubic grains in the as-milled Fe powders, assumed according to the x-ray diffraction profiles analysis (see figure 2). Due to such particle shape a volume packing fraction as well as areas of direct intercrystalline contact in agglomerates are much larger than for spherical grains. This leads to much stronger magnetic correlations and results in softer magnetic behaviour of the as-milled powder than is typically observed for nanostructured Fe with spherical grains and an oxidized surface layer. However, in the samples of Fe particles produced and prepared under high vacuum and consolidated under high pressure [13], the increase of their packing fraction and substantially reduced oxidation enhances the magnetic coupling between particles to the extent that the observed coercivity became as low as the one found in this paper. An important role in this coupling is played also by the A_{in} exchange constant. Considering that for samples studied in this work the hyperfine parameters of the interfaces cannot be distinguished from those of pure Fe, it can be expected that $A_{\mathrm{in}} \approx A_{\mathrm{b}}$, which additionally ensures strong magnetic correlations between the grains. In this case relation (2) interpolates to the uniform case $A_{\mathrm{eff}} \approx A_{\mathrm{b}}$ and does not in practice depend on the microstructural parameters.

At low temperatures a magnetic hardening occurs for the powders milled for 48 h $\geqslant t_{\mathrm{m}} >$ 10 h. It is accompanied by a strong dependence of $M_{\mathrm{ZFC}}(T)$ and a simultaneous increase of the irreversibility. This behaviour resembles the features characteristic of a re-entrant spin glass and could indicate that upon cooling a transition from the ferromagnetic state to a frozen disordered state occurs. For as-milled nanocrystalline Fe a low temperature spin-glass-like state, that can be erased by applying an external field of 1000 Oe, has already been postulated by Del Bianco *et al* [32, 33]. However, it is important to emphasize that the other possible mechanisms that could be responsible for the observed low field ZFC–FC irreversibility were not considered in these papers. The low temperature disordered state of the ball milled nanocrystalline Fe with its collective dynamic behaviour was reported by Bonetti *et al* [17] and ascribed to the spin-glass-like properties of the interfaces. However, for the as-milled powders (48 h $\geqslant t_{\mathrm{m}} >$ 10 h) studied in this work, besides the ZFC–FC irreversibility observed at low fields, the other features characteristic of dynamical properties of the disordered systems (in particular in the ac susceptibility measurements) are not revealed. Moreover, the irreversibility effects already disappear at 500 Oe (figure 5(b)). Thus these results suggest that the ferromagnetic order within the particle agglomerates is due to the strong magnetic correlations between particles across the interfaces. This ferromagnetic order is preserved at low temperatures and the enhanced irreversibility observed in ZFC–FC curves at 50 Oe is simply attributed to the magnetic hardening and arises when the coercive field approaches the applied field. In the framework of the random anisotropy model the increase of the coercivity at low temperatures indicates that the local anisotropy increases faster than the exchange stiffness constant. It can be expected that such changes will be more significant in the topologically disordered interfacial layers and result in a certain reduction of the magnetic correlations between particles.

4.2. Nanocrystalline Fe/FeO system ($t_m = 64$ h)

Prolongation of the milling time to 64 h results in slight oxidation of the Fe particles and formation of an FeO phase, as identified in the Mössbauer spectra (see the inset in figure 4). Although the relative content of this phase is small (∼3%), it causes a significant modification of the overall magnetic behaviour of Fe nanoparticles. FeO phase, which in the bulk form is an antiferromagnet with the transition temperature $T_N \approx 200$ K, is seen in ZFC–FC curves taken at 500 Oe as a small cusp at around 220 K (see the inset in figure 5(b)). This temperature is somewhat higher than the transition temperature of bulk stoichiometric wüstite; this difference can arise from a small enrichment of FeO in iron due to formation of this phase in the oxygen-poor atmosphere and the proximity of ferromagnetic Fe phase. The most prominent feature attributed to the structural changes in this sample is the appearance of dynamic effects which manifest themselves in the ac susceptibility results by a rapid decrease of the real component at low temperatures and a well defined peak in the imaginary component (see figure 8). The occurrence of the FeO phase leads also to magnetic hardening of the powder, the appearance of the peak in the temperature dependences of the coercivity and remanence (figure 7(b)) as well as exchange bias phenomena, typically observed in ferromagnetic–antiferromagnetic nanostructures [34, 35]. Cooling of the sample through the Néel temperature of FeO in the applied field of 1 T down to 5 K causes a shift of the loop towards negative fields by around 70 Oe. This shift is essentially smaller than the exchange field parameter found by Del Bianco *et al* [36], $H_{ex} \approx 450$ Oe, for an Fe–Fe oxide granular system where the fraction of the oxide phase was so large that the Fe grains were considered as being embedded in an oxide matrix, but is similar to the one found by Löffler *et al* [13] for as-prepared compacted Fe particles with low oxygen content.

All the experimental results obtained indicate a collective freezing of the disordered magnetic moments upon cooling, similar to a spin-glass-like transition; $T_f \approx 60$–75 K can be considered as a freezing temperature. In the 64 h milled sample the magnetically disordered state is a result of the disorder of surface/interface spins (enhanced by the antiferromagnetic oxide phase and its coupling to the disturbed ferromagnetic grain shells) as well as dipolar interparticle interactions which are anisotropic in nature and in this sample coexist with the exchange interactions. The spin-glass-like behaviour of fine particles is a quite typical feature of concentrated systems; see e.g. ([5] and references therein). In this case the thermal dependence of the saturated thermoremanent magnetization M_{TR} can be described by an exponential dependence of the type [37]

$$M_{TR}(T) = M_{TR}(0)\exp(-\beta T). \tag{3}$$

A semi-logarithmic plot of the thermoremanent magnetization data collected after cooling the sample at 1 T is shown in figure 9. One can distinguish three temperature regions in which the TRM follows the exponential relaxation behaviour but with different values of the β coefficient: β(4–50 K) = 0.0233; β(75–210 K) = 0.0045; β(230–300 K) = 0.002. The low temperature change of slope (∼62 K) corresponds to the freezing temperature T_f of the disordered magnetic moments of randomly oriented particles and interfacial regions, consistent with a spin-glass-like state at low temperature. In turn, the change of slope observed at ∼224 K corresponds to the small cusp in the ZFC–FC curves and is attributable to the Néel temperature of the FeO phase below which the irreversibility effects as well as the relaxation processes are associated with the enhanced coupling between particles and collective blocking of magnetically coupled regions with a broad distribution of their relaxation times.

The changes in the microstructure of the sample milled for 64 h cause its magnetic hardening. As the average particle diameter remains almost the same as for the previous samples (as seen in figure 3), two main factors are responsible for the observed increase of

the coercivity: (i) strong surface/interface anisotropy and (ii) the reduction of the exchange stiffness constant in the interface A_{in} (and thus the reduction of the effective exchange constant A_{eff}—see equation (2))—both related to the antiferromagnetic oxide layer and the induced enhanced spin disorder. These changes result in a suppression of the exchange correlation length L and, consequently, in magnetic hardening. It is worth noting that any enhancement of the coercivity is seen at temperatures above the Néel temperature of FeO although this transition should result in a certain decoupling between the grains. This is again in agreement with the generalized random anisotropy model [31] which allows discontinuities of magnetization across grain boundaries and includes the possibility of a number of weak intergrain couplings without losing the magnetic interparticle correlations.

5. Conclusions

The low energy milling of microcrystalline Fe under an argon atmosphere and in well controlled conditions gives pure single-phase iron nanostructured powders with crystalline grain size of around 11 nm. Pseudo-cubic shape of the structural domains is assumed since it approximates better the x-ray diffraction profiles; however, no direct observations of the sample microstructure are provided. A certain disorder at the grain boundaries of these particles that extends only over around 0.8 nm can be detected; however, the properties of the interfacial layer, including the hyperfine parameters, cannot be distinguished from those of bulk Fe. It is important to emphasize that the same thickness and a certain topological disorder were recently predicted from a numerical approach based on the embedded atom method [38]. Such a description is consistent with the present experimental features.

The particles form agglomerates where the long range ferromagnetic correlation of exchange coupled grains extending across the grain boundaries leads to a reduction of the effective anisotropy. The soft magnetic behaviour of the as-milled pure iron powder can well be described by the generalized random anisotropy model. In this respect, the most significant role in the effective reduction of the coercivity (which is almost one order of magnitude smaller than that typically observed for surface oxidized Fe particles agglomerates) is played by the strong exchange coupling across the grain boundaries. For the samples considered, the pseudo-cubic shape of the grains results in a high volume packing fraction and large areas of direct intercrystalline contacts. This additionally enhances the interparticle interactions (although for spherical grains with a wide distribution of particle diameters and high packing fractions, similar strong long range ferromagnetic correlations can be achieved, as can be seen in [13]). The ferromagnetic network of correlated particles is preserved at low temperatures and is not disturbed by any spin-glass-like freezing processes, typical of agglomerates of passivated Fe grains. However, a slight magnetic hardening is observed upon cooling which indicates an increase of the local anisotropy, most probably in the topologically disordered grain boundaries.

Slight oxidation of Fe grains with FeO during prolonged milling essentially modifies the overall magnetic behaviour of the powder. The coupling between the spins from the antiferromagnetic oxide layer and those from the topologically disordered grain boundaries leads to frustrated magnetic interactions, giving rise to non-collinear spin structure in the interface. This causes the suppression of the exchange interparticle correlations enhancing simultaneously long range dipolar interactions. The interface spin disorder and the complex state of the interparticle interactions are sources of dynamic effects and spin-glass-like behaviour of such Fe–FeO nanostructures.

Thus the results obtained show that the spin-glass-like behaviour is not an inherent feature of the nanocrystalline state, as postulated by Del Blanco *et al* [33], since pure nanocrystalline Fe powder exhibits a simple ferromagnetic ordering down to 4 K despite a certain topological

disorder at particle surfaces. The effects of collective disordered magnetization freezing in nanoparticle systems require essentially disturbed structure as well as magnetic ordering of the interfacial layer and usually originate from the oxidation and/or incorporated impurities of particle shells.

Acknowledgment

This work was supported by the France–Poland grant (CNRS-PAS Project No 16710/04-05).

References

[1] Herr U, Jing J, Birringer R, Gonser U and Gleiter H 1987 *Appl. Phys. Lett.* **50** 472
[2] Campbell S J and Gleiter H 1993 *Mössbauer Spectrometry Applied to Magnetism and Materials Science* vol 1, (New York: Plenum) pp 241–303
[3] Hernando A and Gonzalez A 2001 *J. Non-Cryst. Solids* **287** 256
[4] Campbell S J, Chadwick J, Pollard R J, Gleiter H and Gonser U 1995 *Physica* B **205** 72
[5] Batlle X and Labarta A 2002 *J. Phys. D: Appl. Phys.* **35** R15
[6] Gangopadhyay S, Hadjipanayis G C, Shah S I, Sorensen C M, Klabunde K J, Papaefthymiou V and Kostikas A 1991 *J. Appl. Phys.* **70** 5888
[7] Gangopadhyay S, Hadjipanayis G C, Dale B, Sorensen C M, Klabunde K J, Papaefthymiou V and Kostikas A 1992 *Phys. Rev.* B **45** 9778
[8] Bødker F, Mørup S and Linderoth S 1994 *Phys. Rev. Lett.* **72** 282
[9] Linderoth S, Morup S and Bentzon M D 1995 *J. Mater. Sci.* **30** 3142
[10] Del Bianco L, Hernando A, Bonetti E and Navarro E 1997 *Phys. Rev.* B **56** 8894
[11] Del Bianco L, Fiorani D, Testa A M, Bonetti E and Signorini L 2002 *Phys. Rev.* B **66** 174418
[12] Balogh J, Bujdoso L, Kaptas D, Kemeny T, Vincze I, Szabo S and Beke D L 2000 *Phys. Rev.* B **61** 4109
[13] Löffler J F, Meier J P, Doudin B, Ansermet J P and Wagner W 1998 *Phys. Rev.* B **57** 2915
[14] Zhang X X, Liu H, Fung K K and Qin B X 2000 *Physica* B **279** 185
[15] Ślawska-Waniewska A and Greneche J M 1997 *Phys. Rev.* B **56** R8491
[16] Del Bianco L, Ballesteros C, Rojo J M and Hernando A 1998 *Phys. Rev. Lett.* **81** 4500
[17] Bonetti E, Del Bianco L, Fiorani D, Rinaldi D, Caciuffo R and Hernando A 1999 *Phys. Rev. Lett.* **83** 2829
[18] Eckert J, Holzer J C, Krill C E and Johnson W L 1992 *J. Mater. Res.* **7** 1751
[19] Balogh J, Kemeny T, Vincze I, Szabo S, Beke D L and Toth J 1999 *Phys. Rev.* B **59** 14786
[20] Suryanarayana C 2001 *Prog. Mater. Sci.* **46** 1
[21] Börner I and Eckert J 1997 *Mater. Sci. Eng.* A **226–228** 541
[22] Lutterotti L and Scardi P J 1990 *J. Appl. Crystallogr.* **23** 246–52
[23] Bonetti E, Del Bianco L, Pasquini L and Sampaolesi E 1998 *Nanostruct. Mater.* **10** 741–53
[24] Guérault H and Greneche J-M 2000 *J. Phys.: Condens. Matter* **12** 4791–8
[25] Guérault H, Bureau B, Silly G, Buzaré J Y and Greneche J M 2001 *J. Non-Cryst. Solids* **287** 65–9
[26] Ding J, Miao W F, McCormick P G and Street R 1998 *J. Magn. Magn. Mater.* **177–181** 933
[27] Zhao Y H, Sheng H W and Lu K 2001 *Acta Mater.* **49** 365
[28] Peng D L, Hihara T, Sumiyama K and Morikawa H 2002 *J. Appl. Phys.* **92** 3075
[29] Ślawska-Waniewska A, Roig A, Gich M, Casas Ll, Racka K, Nedelko N and Molins E 2004 *Phys. Rev.* B **70** 054412
[30] Choi C J, Dong X L and Kim B K 2001 *Scr. Mater.* **44** 2225
[31] Löffler J F, Braun H B and Wagner W 2000 *Phys. Rev. Lett.* **85** 1990
[32] Del Bianco L, Bonetti E, Fiorani D, Rinaldi D, Caciuffo R and Hernando A 2001 *J. Magn. Magn. Mater.* **226–230** 1478
[33] Del Bianco L, Hernando A and Fiorani D 2002 *Phys. Status Solidi* a **189** 533
[34] Kodama R H, Berkowitz A E, McNiff E J Jr and Foner S 1996 *Phys. Rev. Lett.* **77** 394
[35] Kodama R H, Makhlouf S A and Berkowitz A E 1997 *Phys. Rev. Lett.* **79** 1393
[36] Del Bianco L, Fiorani D, Testa A M, Bonetti E and Signorini L 2004 *Phys. Rev.* B **70** 052401
[37] Dormann J L, Fiorani D, Tholence J L and Sella C 1983 *J. Magn. Magn. Mater.* **35** 117
[38] Grafouté M, Labaye Y, Calvayrac F and Grenèche J M 2005 *Eur. Phys. J.* B **45** 419